

Superconducting transition of a two-dimensional Josephson junction array in weak magnetic fields

In-Cheol Baek, Young-Je Yun, Jeong-Il Lee, and Mu-Yong Choi

*BK21 Physics Division and Institute of Basic Science,
Sungkyunkwan University, Suwon 440-746, Korea*

Abstract

The superconducting transition of a two-dimensional (2D) Josephson junction array exposed to weak magnetic fields has been studied experimentally. Resistance measurements reveal a superconducting-resistive phase boundary in serious disagreement with the theoretical and numerical expectations. Critical scaling analyses of the IV characteristics indicate contrary to the expectations that the superconducting-to-resistive transition in weak magnetic fields is associated with a melting transition of magnetic-field-induced vortices directly from a pinned-solid phase to a liquid phase. The expected depinning transition of vortices from a pinned-solid phase to an intermediate floating-solid phase was not observed. We discuss effects of the disorder-induced random pinning potential on phase transitions of vortices in a 2D Josephson junction array.

PACS numbers: 74.25.Qt, 74.81.Fa, 74.25.Dw, 64.60.Cn

When a two-dimensional (2D) Josephson junction array (JJA) is immersed in a perpendicular magnetic field, a finite density of vortices are induced in the array. The competition between the repulsive vortex-vortex interaction and the attractive periodic pinning potential due to the discreteness of the array results in interesting forms of superconducting-resistive phase boundaries as functions of a magnetic field¹. The superconducting-to-resistive transition in strong magnetic fields or at high vortex densities has been discussed in terms of the melting of a vortex solid pinned to an underlying lattice.^{2,3,4,5} On the other hand, the superconducting-to-resistive transition in weak magnetic fields or at low vortex densities was found in simulation studies to be associated with the depinning transition of a pinned vortex solid, the appearance of which was predicted by Nelson and Halperin⁶ in late 70s. Monte Carlo (MC) simulations of the lattice Coulomb gas model for vortices⁷ showed that for a vortex density, the number of flux quanta per plaquette, $f < 1/25$ the pinned vortex solid transforms into a vortex liquid through two successive phase transitions: a depinning transition from a pinned solid to a floating solid at a lower temperature T_p , approximately linear in f , and a melting transition from a floating solid to a liquid at a higher temperature $T_m \sim 0.045J/k_B$, approximately independent of f , in which J is the Josephson coupling energy per junction. For $f \gtrsim 1/25$, both transitions were found to appear at the same temperature increasing with f . These results have been confirmed semiquantitatively by different numerical or analytical studies of related models such as the XY model⁸, the resistively-shunted-junction model⁹, and the continuum model of a Coulomb gas in a periodic potential¹⁰. While the existence of an intermediate hexatic phase just above the melting point has been also predicted by theory^{6,11}, no evidence was found in the numerical studies.

Despite the agreement among the theoretical and numerical efforts, the experimental confirmation of the appearance of a depinning transition in the weak field limit has yet to be done. We, therefore, investigated experimentally the superconducting transition of a JJA in weak magnetic fields. The measurements of the resistance and the current-voltage (IV) characteristics of a square array represent a phase diagram in serious disagreement with the theoretical and numerical expectations. The expected depinning transition was not observed. We discuss effects of the disorder-induced random pinning potential on phase transitions of vortices in a 2D JJA.

The experiments were performed on a square array of 400×600 Nb/Cu/Nb Josephson junctions. Cross-shaped $0.2\text{-}\mu\text{m}$ -thick Nb islands, fabricated by applying photolithography

and reactive-ion etching to the Nb/Cu double layer, were disposed on a 0.3- μm -thick Cu film periodically with a lattice constant of 13.7 μm , a junction width of 4 μm , and a junction separation between adjacent sites of 1.5 μm . The photograph of Fig. 1(a) shows the structure of the JJA sample used in this work. The variation of the junction separation in the sample was less than 0.1 μm . The standard four-probe technique was adopted for the measurements of the resistance and the IV characteristics. The current and voltage leads were attached to the Cu layer. The current leads were connected 3 mm away from the ends of the array to improve the uniformity of the injected current. Voltage leads were placed 100 junctions away from the end edges of the array so that there exist 400×400 junctions between the voltage leads. The sample voltage was measured by a transformer-coupled lock-in amplifier with a square-wave current at 23 Hz. The single-junction critical current i_c at low temperatures can be obtained directly from the IV curve. At low temperatures, the slope dV/dI of the curve has its maximum at a current equal to i_c multiplied by the number of Nb islands perpendicular to the current direction. The i_c and the junction coupling strength $J(= \hbar i_c/2e)$ at high temperatures were determined by extrapolating the i_c vs T data at low temperatures by the use of the de Gennes formula for a proximity-coupled junction in the dirty limit, $i_c(T) = i_c(0)(1 - T/T_{co})^2 \exp(-\alpha T^{1/2})$, where T_{co} is the BCS transition temperature. We have also tried another formula developed by Zaikin and Zharkov¹² and found both formulas generate practically the same i_c 's for our sample at the temperatures of interest. Representing the superconducting transition temperatures of the sample in units of J/k_B by using the i_c 's determined with the de Gennes formula, they are 0.85 for $f = 0$ and 0.42 for $f = 1/2$. These values are lower by 5-7% than the superconducting transition temperature (T_c 's) found from many numerical studies, which are 0.89 for $f = 0$ and 0.45 for $f = 1/2$ ¹³. This demonstrates that $i_c(T)$ of the sample determined with the formulas is accurate within 10% of error. During the measurements, the temperature was controlled by a Lake Shore 340 temperature controller with fluctuations less than 1 mK. A solenoid generated external magnetic fields in the sample space where ambient magnetic fields were screened out by μ -metal. The magnetic field or the vortex density was adjusted from the magnetoresistance measurements of the sample with 50- μA excitation current. The presence of distinct resistance minima at fractional f 's in the magnetic field vs resistance curve made precise adjustment of the vortex density possible.

Figure 1(c) shows the sample resistance with 30- μA excitation current as a function of

f at $T = 3.59$ K. The appearance of many pronounced higher-order dips indicates the good uniformity of the magnetic field over the sample. The magnetoresistance curve is impressively similar to the mean-field superconducting-resistive phase boundary numerically predicted in Ref. 1. The curve exposes, as numerically predicted, that the mean-field superconducting transition temperature T_{MF} is a decreasing function of f in the low f region. As stated above, T_c as an increasing function of f was observed in the same region in the MC simulations. Even though a mean-field phase diagram does not always resemble the real one, the f -dependence of T_{MF} of our sample raises a question about validity of the phase diagram from the MC simulations. In order to examine the f -dependence of T_c of a JJA in weak magnetic fields, we measured the sample resistance R as functions of the temperature T for six different vortex densities $f = 1/50, 1/36, 1/25, 1/16, 1/10$, and $1/8$. Figure 2 shows some of the T vs R traces. The superconducting transition temperature T_c determined from the T vs R curves is plotted against f in Fig. 3. The superconducting-resistive phase boundary differs from the theoretical and numerical expectations summarized above. T_c decreases with f increased, contrary to the numerical observations. The T_c at $f = 1/50$ is ~ 0.32 in units of J/k_B , which is ~ 10 times the numerical value of T_p and ~ 7 times that of T_m . The T_c 's at $f = 1/50, 1/36$, and $1/25$ exceed even the melting temperatures of densely populated vortices for $f = 2/5, 1/3$, and $1/5$ ^{4,5,14}. Such high T_c 's appear hardly reconcilable with the proposed depinning transition, but possibly with the melting transition of a pinned vortex solid as for dense vortex systems.

The gradual drop of the resistance of the sample upon approaching the transition indicates that the observed superconducting transitions are all continuous phase transitions. For a continuous superconducting transition, the critical scaling analysis of the IV characteristics may provide valuable information about the nature of the superconducting transition. Figure 4 displays the IV characteristics of the sample for $f = 1/50, 1/36$, and $1/16$. The $\log I$ vs $\log V$ isotherms were obtained by averaging 15-240 measurements for each value of current. The derivative $d(\log V)/d(\log I)$, that is, the slope of the IV curves of Fig. 4 as functions of I are in Fig. 5. The data at high currents are due to the single-junction effect and thus should be left out of consideration. The derivative plots show that for all the f 's studied, the IV curves have negative curvatures at low temperatures. At high temperatures, they have positive curvatures. The high-temperature and low-temperature curves are separated by a straight line satisfying the power-law IV relation. Thermally activated vortex

motion would give rise to Ohmic IV characteristics in the low current limit and positive curvature in IV curves at intermediate currents. Negative curvature in the low- T curves implies vanishing resistance in the low current limit, indicating a superconducting state as the low-temperature state. The IV characteristics thus indicate that for the f 's, the JJA undergoes a continuous superconducting transition at the temperature where a straight IV curve appears. A detailed scaling theory¹⁵ suggests that for a continuous superconducting transition, the IV characteristics in 2D should scale as $V/I|T - T_c|^{z\nu} = \mathcal{E}_{\pm}(I/T|T - T_c|^{\nu})$, where ν and z are critical exponents and \mathcal{E}_{\pm} the scaling functions above and below T_c . This scaling form becomes a simple power-law IV relation, $V \sim I^{z+1}$, at $T = T_c$. Thus, one may find T_c and the dynamic critical exponent z directly from the straight $\log I$ vs $\log V$ isotherm. The correlation-length exponent ν can be obtained from the scaling analysis of the IV data. Although the scaling analysis of IV data is an effective tool for studying the critical behaviors of superconductors, special care should be taken not to extract any false information from the analysis. It has been recently shown for cuprate superconductors that the good data collapse can be achieved for a wide range of T_c and critical exponents and sometimes does not even prove the existence of a phase transition.¹⁶ It has been also shown that both the current noise¹⁷ and the finite-size effect¹⁸ may create Ohmic behavior at low currents even below the superconducting transition and lead to an underestimate of T_c and incorrect ν and z . The IV data in Fig. 4, however, do not suffer such complications. We avoided the current-noise problem by employing the phase-sensitive signal-detection method using a low-frequency square-wave current as described above. The effect of finite-size-induced free vortices was also found insignificant for JJA samples exposed to a magnetic field.⁵ The IV curves in Fig. 4 prove that the large flexibility in determining the critical exponents and temperature from IV data is not the case for the array sample. Unlike the IV data of cuprate superconductors, the IV curves of the array exhibit evident concavities below the transition. One can determine T_c with uncertainty $\Delta T_c \approx \pm 0.1$ K from the curves. The T_c 's determined from the straight IV curves agree within the uncertainties with those from the T vs R data. In the process of the scaling analysis, the distinct concavities of the IV curves further reduce the arbitrariness in determining T_c to ± 0.5 - 0.7 K. The IV data scaled on the basis of the scaling form with T_c and z derived from the straight IV curves are shown in Fig. 6. Each plot contains IV curves at 18-19 different temperatures. The scaling plots confirm that the JJA at the f 's studied undergoes a continuous superconducting phase transition

at the temperature where a straight IV curve appears. The insets of Fig. 6 exhibit the values of T_c , ν , and z used to scale the data. The T_c 's derived from the scaling analyses are in accordance within experimental errors with those from the resistance measurements. For all three f 's, the dynamic critical exponent z is less than 1 and the correlation-length exponent ν is much larger than the 2D Ising value ($\nu_I = 1$). The low-temperature IV curves can be fitted into the form $V \sim I \exp[-(I_T/I)^\mu]$ with $\mu = 0.7$ -1.1. The scaling behaviors of the IV characteristics are quite similar to those found for $f = 2/5$, $1/3$, and $1/5^5$, for which the superconducting transition is understood in terms of melting of a pinned vortex solid driven by domain-wall excitations^{3,4,5}. The large low-current voltage signals near the transition also appear to be compatible with the melting transition at $T = T_c$. A floating solid is expected to be much less mobile near the transition and thus generate much lower voltage signal than melted vortices. Taking into consideration of the low vortex densities of our systems, the low-current voltage signals near the transition are as large as those of melted vortices for $f = 2/5$, $1/3$, and $1/5$ reported in Ref. 5. The large voltage signals above the transition, the scaling behaviors of the IV data, and the high T_c 's, all indicate that the observed superconducting transitions in the weak magnetic fields are associated with the melting transition of a pinned vortex-solid to a vortex liquid without passing through an intermediate floating solid phase.

The high melting transition temperatures and the absence of a depinning transition are in serious disagreement with the theoretical and numerical expectations. The disagreement in weak magnetic fields contrasts with the agreement in strong magnetic fields. For $f = 2/5$, the same sample exhibited a superconducting transition at about the same temperature as observed in simulations. It has been recently found in numerical studies of the 2D Coulomb gas¹⁹ that the floating vortex-solid phase may exist only in small arrays. This may explain the absence of a floating solid phase in our large array sample, but not the high melting temperatures. We therefore consider the disorder-induced random pinning potential as a possible cause for the disagreement in weak magnetic fields. The numerically obtained phase diagram^{7,10} intimates that the depinning and melting transitions may appear at the same temperature when the depinning temperature T_p exceeds the melting temperature T_m . A higher T_p can be achieved with stronger pinning of vortices to the underlying lattice. In the process of fabricating a JJA sample, random variation of the junction coupling strength is inevitably introduced. The inevitable variation of junction coupling strength in a real array

may provide additional pinning and an enhanced T_c for vortices dislocated from the periodic disposition. Such an effect of random bond disorder on T_c should be much weaker in strong magnetic fields, consistent with the observations, because when densely populated vortices are dislocated from the periodic disposition, the increment of the repulsive vortex-vortex interaction energy effectively countervails the contribution of the random pinning potential. The variation of the coupling strength in our sample estimated from the I vs dV/dI curve in Fig. 1(b) is $\lesssim \pm 15\%$. Yet it is not quite certain whether such an amount of variation of the coupling strength can raise T_c so much. In order to ascertain whether extra random pinning can raise T_c so effectively in weak magnetic fields, we measured resistively the T_c of a system with artificially introduced random pinning. Figure 7 shows the T_c as a function of f for a square JJA in which 14% of superconducting islands are randomly diluted. This site-diluted sample also contains the inevitable bond disorder, that is, the variation of junction coupling strength as much as the foregoing sample. We find in the figure that the random site disorder affects the T_c of a JJA as presumed above. The T_c in units of J/k_B for $f = 1/50$ - $1/8$ was elevated by the addition of site-disorder by 47-100% above that of the foregoing sample. For $f = 2/5$, the change of T_c was found less than 5%. The superconducting behavior of the site-diluted sample proves that the random pinning potential induced by disorder is quite effective in stabilizing the superconducting vortex-solid phase in weak magnetic fields.

In summary, the measurements of the resistance and the IV characteristics disclosed a phase diagram of a JJA exposed to weak magnetic fields in sharp contrast to the theoretical and numerical expectations. Vortices in a square array at $f = 1/50$ - $1/8$ were found to undergo a melting transition directly from a pinned-solid phase to a liquid phase at $T_c \sim 0.15$ - $0.32 J/k_B$, ~ 3 - 7 times the predicted melting temperature. The expected depinning transition was not observed. The experiments on the site-diluted array reveal that the disorder-induced random pinning can stabilize the superconducting pinned-solid phase in weak magnetic fields even at 10 times the melting temperature of a disorder-free system and is probably responsible for the experimental findings contrary to the theoretical expectations.

This work was supported by the BK 21 program of the Ministry of Education.

¹ Y.-L. Lin and F. Nori, Phys. Rev. B **65**, 214504 (2002); Q. Niu and F. Nori, *ibid.* **39**, 2134 (1989), and references therein.

- ² S. Teitel and C. Jayaprakash, Phys. Rev. B **27**, 598 (1983); Y.-H. Li and S. Teitel, Phys. Rev. Lett. **65**, 2595 (1990).
- ³ X. S. Ling, H. J. Lezec, M. J. Higgins, J. S. Tsai, J. Fujita, H. Numata, Y. Nakamura, Y. Ochiai, Chao Tang, P. M. Chaikin, and S. Bhattacharya, Phys. Rev. Lett. **76**, 2989 (1996).
- ⁴ C. Denniston and C. Tang, Phys. Rev. Lett. **79**, 451 (1997); Phys. Rev. B **60**, 3163 (1999).
- ⁵ Young-Je Yun, In-Cheol Baek, and Mu-Yong Choi, Phys. Rev. Lett. **89**, 037004 (2002).
- ⁶ D. R. Nelson and B. I. Halperin, Phys. Rev. B **19**, 2457 (1979).
- ⁷ M. Franz and S. Teitel, Phys. Rev. B **51**, 6551 (1995); V. Gotcheva and S. Teitel, Phys. Rev. Lett. **86**, 2126 (2001).
- ⁸ S. A. Hattel and J. M. Wheatley, Phys. Rev. B **51**, 11 951 (1995).
- ⁹ V. I. Marconi and D. Domínguez, Phys. Rev. B **63**, 174509 (2001).
- ¹⁰ J. P. Straley, A. Y. Morozov, and E. B. Kolomeisky, Phys. Rev. Lett. **79**, 2534 (1997).
- ¹¹ J. P. Rodriguez, Phys. Rev. Lett. **87**, 207001 (2001).
- ¹² A. D. Zaikin and G. F. Zharkov, Fiz. Nizk. Temp. **7**, 375 (1981) [Sov. J. Low Temp. Phys. **7**, 184 (1981)].
- ¹³ E. Granato and M. P. Nightingale, Phys. Rev. B **48**, 7438 (1993); S. Lee and K.-C. Lee, *ibid.* **49**, 15 184 (1994); P. Olsson, Phys. Rev. Lett. **75**, 2758 (1995); J. V. José and G. Ramirez-Santiago, *ibid.* **77**, 4849 (1996), and references therein.
- ¹⁴ Y.-H. Li and S. Teitel, Phys. Rev. Lett. **67**, 2894 (1991).
- ¹⁵ D. S. Fisher, M. P. A. Fisher, and D. A. Huse, Phys. Rev. B **43**, 130 (1991).
- ¹⁶ D. R. Strachan, M. C. Sullivan, P. Fournier, S. P. Pai, T. Venkatesan, and C. J. Lobb, Phys. Rev. Lett. **87**, 067007 (2001); D. R. Strachan, C. J. Lobb, and R. S. Newrock, Phys. Rev. B **67**, 174517 (2003).
- ¹⁷ M. C. Sullivan, T. Frederiksen, J. M. Rapaci, D. R. Strachan, R. A. Ott, and C. J. Lobb, Phys. Rev. B **70**, 140503(R) (2004).
- ¹⁸ J. Holzer, R. S. Newrock, C. J. Lobb, T. Aouaroun, and S. T. Herbert, Phys. Rev. B **63**, 184508 (2001); K. Medvedyeva, B. J. Kim, and P. Minnhagen, *ibid.* **62**, 14 531 (2000); S. W. Pierson, M. Friesen, S. M. Ammirata, J. C. Hunnicutt, and L. A. Gorham, *ibid.* **60**, 1309 (1999).
- ¹⁹ C. E. Creffield and J. P. Rodriguez, Phys. Rev. B **67**, 144510 (2003).

FIG. 1: (a) Photograph of the square Josephson junction array used in the experiment. (b) I vs dV/dI at $T = 3.10$ K. (c) Sample resistance with $30\text{-}\mu\text{A}$ excitation current as a function of the vortex density f at $T = 3.59$ K.

FIG. 2: Temperature dependences of the resistance at $f =$ (a) $1/50$, (b) $1/36$, and (c) $1/16$. The arrows denote where the superconducting transition occurs. The resistance was measured with $3\text{ }\mu\text{A}$ current injected into the sample.

FIG. 3: Vortex-density dependence of T_c determined from the resistance measurements. Note that T_c is in units of J/k_B .

FIG. 4: The IV characteristics for (a) $f = 1/50$ at $T = 3.600\text{-}4.500$ K, (b) $f = 1/36$ at $T = 3.600\text{-}4.500$ K, and (c) $f = 1/16$ at $T = 3.500\text{-}4.400$ K. The dashed lines are drawn to show the power law ($V \sim I^{z+1}$) behavior at the superconducting temperature.

FIG. 5: Current dependences of the slope of the IV curves in Fig. 4. Excessively fluctuating data at low currents are not shown.

FIG. 6: Scaling plots of the IV curves. Each plot contains IV curves at 18-19 different temperatures. The insets show the values of T_c , z , and ν used to scale the data.

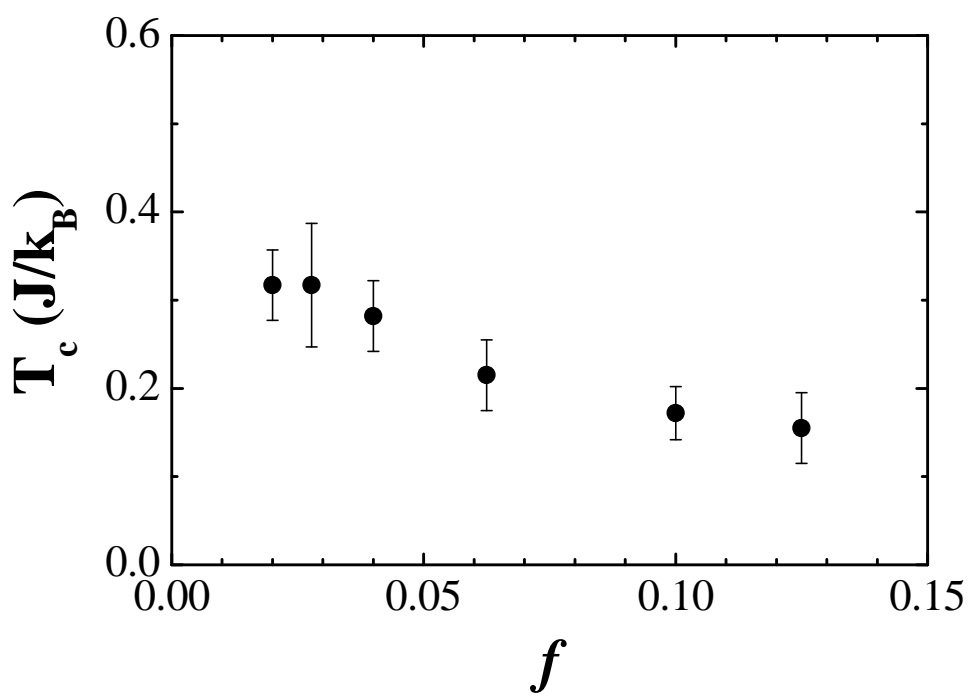
FIG. 7: T_c of the 14% site-diluted sample as a function of vortex density.

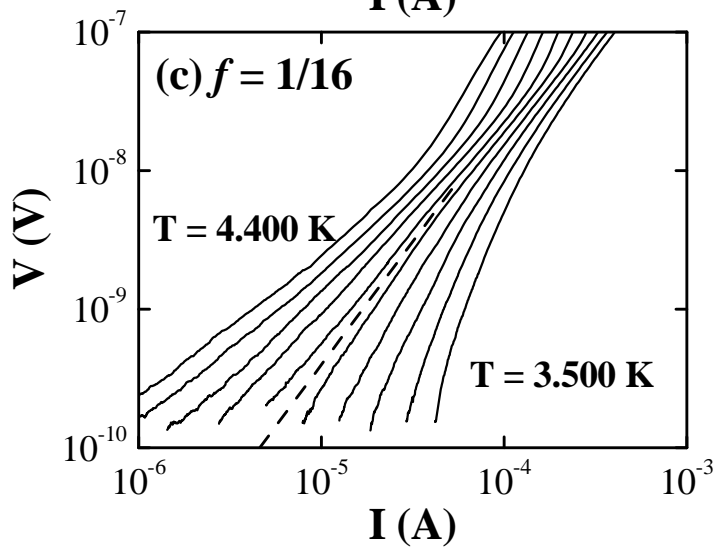
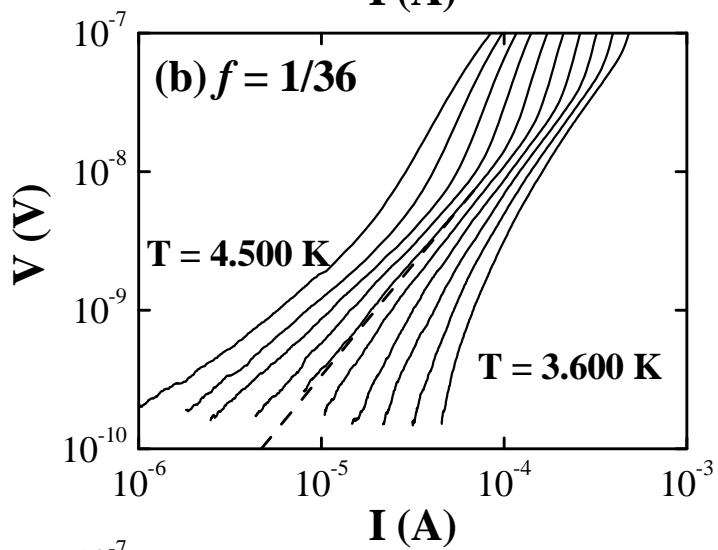
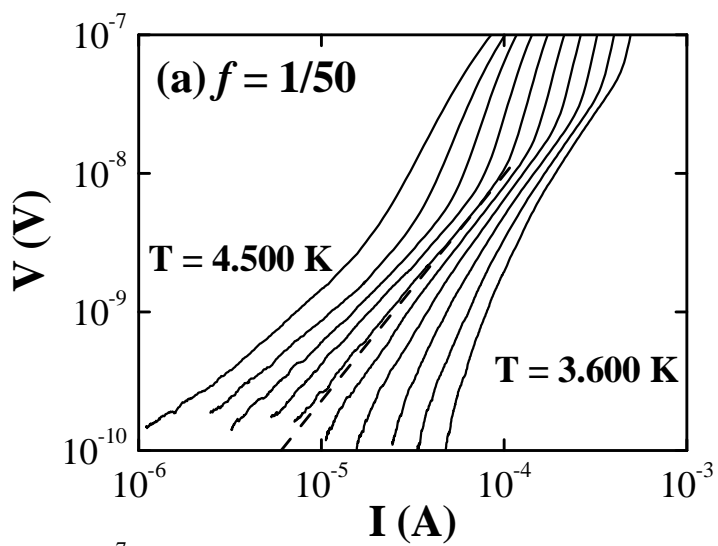
This figure "fig1.JPG" is available in "JPG" format from:

<http://arxiv.org/ps/cond-mat/0506259v1>

This figure "fig2.JPG" is available in "JPG" format from:

<http://arxiv.org/ps/cond-mat/0506259v1>





This figure "fig5.JPG" is available in "JPG" format from:

<http://arxiv.org/ps/cond-mat/0506259v1>

